Preprints of the 23rd IFAC World Congress
Busan, Republic of Korea, August 23-28, 2026

# Event-Triggered Neural Network-Based Adaptive Cruise Control ⋆

**Yanan Zhang** *, **Jiacheng Song** * **Peilun Ju** **

* *College of Mechanical and Electronic Engineering, Northwest A&F University, Yangling, 712100, People's Republic of China (e-mail: ynzhang@nwafu.edu.cn; jiacheng.song@nwafu.edu.cn).*
** *School of Economics and Management, Chang'an University, Xi'an, 710064, People's Republic of China (e-mail: jupeilun@chd.edu.cn).*

**Abstract:** This paper focuses on the nonlinear driving resistance of vehicles and designs an on-demand adaptive cruise control (ACC) algorithm without a precise model. While ensuring safety control, it reduces the execution frequency of the actuator. Firstly, Radial Basis Function Neural Networks (RBF NNs) are used to characterize uncertain driving resistance and reconstruct the nonlinear dynamic model of the vehicle. Secondly, in response to the safety distance target of vehicle adaptive cruise control, a virtual controller is designed using backstepping control technology to convert vehicle distance control into speed control, and a speed feedback controller is designed. Moreover, when designing the speed control term, an event-triggered mechanism is introduced to achieve on-demand control of the actuator, and system stability is analyzed according to Lyapunov theory. Finally, the feasibility and superiority of the designed algorithm were verified using the Economic Commission for Europe (ECE) operating conditions to test the speed curve.

*Keywords:* Adaptive cruise control, radial basis function neural networks, event-triggered control, backstepping control technology

## 1. INTRODUCTION

Adaptive Cruise Control (ACC) collects surrounding environmental data through sensors, automatically adjusts driving speed, and ensures a safe distance(Zhu et al., 2024). ACC technology significantly reduces driving load, enhances driving safety, and improves the smoothness of road traffic, thus becoming a focus of research in the field. The research on ACC has made significant progress in multiple aspects, including vehicle modeling, distance control, speed control, and so on. However, vehicles may encounter various unpredictable resistances during driving, which makes the task of precise modeling complex (Ju and Song, 2023). In addition, the perception, planning, and other processes of unmanned vehicles require a large amount of computing resources (Yu and Wang, 2022). Therefore, how to design ACC algorithms for vehicles without relying on precise vehicle dynamics models and with limited information will play a crucial role for autonomous vehicles.

Various ACC control algorithms have been proposed, including PID-ACC algorithm (Izci et al., 2022), Sliding Mode Control (SMC) ACC algorithm (Sawant et al., 2020), Model Predictive Control (MPC) ACC algorithm (Lin et al., 2020), model free ACC algorithm (Zhang and Song, 2023),etc. Zhang and Ioannou (2006) used pole placement technology to select parameters in the PID-ACC algorithm, aiming to achieve accurate leader vehicle speed tracking and safe distance control. Milanés et al. (2011) combined fuzzy logic control with intelligent PI control to customize a vehicle stop ACC system for low-speed urban traffic environments. Park and Lee (2017) designed an Linear Quadratic Regulation (LQR) based ACC control algorithm, with a focus on reducing unnecessary acceleration and deceleration to reduce energy waste. Marzbanrad and Karimian (2011) used MPC and adopted a rolling horizon control (RHC) strategy to establish a constrained optimal control problem, thereby obtaining the expected acceleration at any time step. Ganji et al. (2014) studied the SMC-ACC algorithm and demonstrated the effectiveness and superiority of SMC-ACC in control performance than PID-ACC. Derbel et al. (2013) proposed an improved intelligent driver model aimed at improving the safety and stability of ACC. The introduction of this model helps to make ACC more in line with the behavioral characteristics of human drivers, thereby improving driving comfort and safety. These ACC control algorithms each have different characteristics and application scenarios, and suitable algorithms can be selected based on specific application needs. However, above algorithms are all based on periodic rate sampling control, inevitably resulting in actuator control redundancy.

Recently, a novel on-demand control method was proposed, namely Event Triggered Control (ETC), which executes control tasks only when the pre-set triggered conditions are satisfied (Yang et al., 2022). Xu et al.

⋆ This work was supported by the Fundamental Research Funds for the Central University of China under Grants Z1090122053, Z1090124102, the Shaanxi Postdoctoral Science Foundation under Grant 2023BSHYDZZ63, and the Key Research and Development Program of Shaanxi under Grants 2025NC-YBXM-208, 2025NC-YBXM-214.

©2026 the authors. Accepted by IFAC for publication under a Creative Commons Licence CC-BY-NC-ND

(2019) considered the problem of actuator failure in nonlinear systems and proposed an adaptive event triggered control method. They considered total effectiveness loss and partial effectiveness loss , proposed an event triggered mechanism that affects measurement errors, and designed a tracking controller for a single nonlinear system. ETC has been deeply studied in theory and has been proven to be used to reduce control communication and controller update times while ensuring control effectiveness. As a terminal, vehicle has strict requirements for power consumption. When there are high requirements for efficiency, power consumption, and computing power, the more appropriate expression for computing power is GOPS/W or TOPS/W, which refers to the amount of computation that can be completed per unit of watt consumed. 1TOPS represents the processor's ability to perform one trillion operations per second ($10^{12}$). The L2 autonomous driving requires a computing power of 10 TOPS, while the Horizon's Journey 2 computing power is 4 TOPS. If ETC is combined with ACC, it can effectively alleviate the problem of insufficient computing power in vehicle autonomous driving. Therefore, it is necessary to conduct research on ACC algorithms based on ETC.

This paper studied the design of adaptive cruise event triggering algorithms for vehicles that do not rely on precise vehicle models. The main contributions are:

- The designed algorithm utilizes the vehicle's state information to learn the uncertain driving resistance online, requiring only one adaptive learning of network weights;
- Compared to time triggered sampling control, the designed algorithm can significantly reduce the execution frequency of the actuator by introducing an ETC mechanism.

## 2. PROBLEM FORMULATION

### *2.1 Vehicle dynamics*

A longitudinal dynamic model of vehicle can be obtained based on Newton's law:

$$\dot{v}(t) = F/m - \mathcal{F} \tag{1}$$

where $F$ is the power that the vehicle needs to provide; $\mathcal{F} = \frac{1}{2m}C_D A\rho v(t)^2 + gC_R + g\sin(\theta)$ representing the ratio of vehicle running resistance to mass. However, the driving resistance encountered by vehicles is subject to a multitude of influencing factors (weather changes, road conditions, etc.) and parameters ($C_D$, $A$, $\rho$, $C_R$, $\theta$), which have nonlinear and time-varying characteristics. Using RBF NNs to approximate the nonlinear driving resistance, vehicle model is written as:

$$\begin{aligned} \dot{p}(t) &= v(t) \\ \dot{v}(t) &= u(t) + N(\bar{x}) \\ N(\bar{x}) &= W^{*}\Psi(\bar{x}) + \varepsilon(\bar{x}) \end{aligned} \tag{2}$$

where $u(t) = F(t)/M$ is the control input, $\bar{x} = [p, v]$, $W^{*T}$ is the optimal weight vector that minimizes $\varepsilon(\bar{x})$, $|\varepsilon(\bar{x})| \leq \bar{\varepsilon} \leq +\infty$, $\Psi(\bar{x})$ denotes Gaussian functions.

### *2.2 Control objective*

ACC dynamically adjusts its velocity to maintain a proximity to the preceding vehicle, ensuring that the actual distance between them converges towards a predefined distance, as shown in Figure 1.

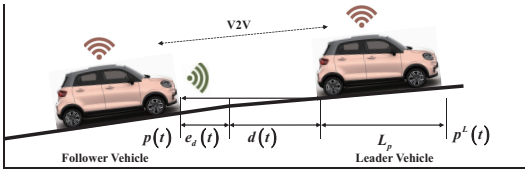



Fig. 1. ACC structure

To achieve the desired distance, define the distance tracking error:

$$e_d(t) = p(t) - p^L(t) + d \tag{3}$$

where $p^L(t)$ denotes the true position of leader vehicle. The goal of ACC is to achieve $e_d(t) \to 0$. $d$ describes the expected vehicle spacing, and $d$ is a constant. The spacing error of vehicles does not take into account the length of the vehicle body $L_P$, mainly because in practical engineering, the distance between two vehicles is directly obtained through sensors. In addition, the length of the vehicle $L_P$ is a constant value, which is zero after differentiation and will not affect the design and stability analysis of the controller.

In addition, traditional time driven control methods require periodic sampling to update and transmit control signals. This sampling method does not consider real-time network resource utilization, and dynamic evolution of the system. When the system is stable, the fluctuation of adjacent sampling points is very small, and sampling at this time will waste a certain amount of system resources. To avoid limitations caused by time driven control, ETC is used to execute control tasks only when the pre-set triggered conditions are satisfied in this paper, which can significantly reduce the number of controller updates. Figure 2 provides a time series explanation of the event triggering mechanism. At each time $(i_k h, i_k = 0, 1, 2, \ldots)$, data is sampled, but only when the triggering conditions are met $(t_k, t_{k+1}, t_{k+2}, \ldots)$, the data is sent to the actuator. The control input is maintained constant through a zero order holder on $t_0 = [t_k, t_{k+1}], t_1 = [t_{k+1}, t_{k+2}]$.

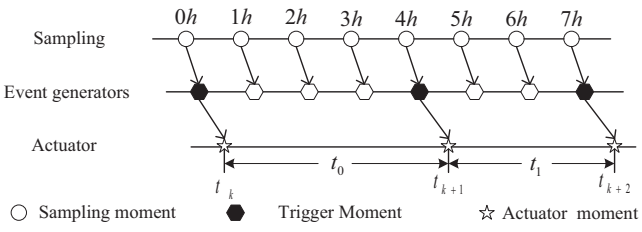



Fig. 2. Event triggering mechanism

This paper aims to integrate ETC technology with ACC to efficiently mitigate the challenge of limited computational resources for autonomous vehicle. The control objective is to design an ETC based ACC that allows the follower to automatically follow the leader safely at the desired

vehicle distance under the influence of uncertain driving resistance. The specific objectives are:

- The actual distance between vehicles tends to be the expected vehicle spacing, and the distance error should be as small as possible, i.e $\lim_{t\to\infty} p(t) - p^L(t) + d \to 0$;
- The following car can quickly respond to changes in the leader car, and the speed error between the two cars should be as small as possible, i.e $\lim_{t\to\infty} \dot{p}^L(t) - \dot{p}(t) \to 0$.

For controller design and stability analysis, the following lemmas are given.

*Lemma 1.* (Song et al., 2019) For any real number $w$, there is a non-negative constant $\epsilon$ such that the following condition holds:

$$0 \leq |w| - \frac{w^2}{\sqrt{w^2+\epsilon^2}} \leq \epsilon \tag{4}$$

*Lemma 2.* (Song et al., 2019) For the given parameters $w_0 > 0$ and $\eta \in \mathbb{R}$, there are inequalities:

$$0 \leq |\eta| - \eta \tanh(\frac{\eta}{w_0}) \leq \kappa w_0 \tag{5}$$

where $\kappa = e^{-(\kappa+1)}$, $\kappa = 0.2785$ is a constant.

## 3. ETC BASED ACC DESIGN

### *3.1 Control algorithm design*

Using backstepping technology to design the controller, its coordinates are transformed into

$$\begin{aligned} e_d(t) &= p(t) - p^L(t) + d \\ e_v(t) &= v(t) - \alpha_d(t) \end{aligned} \tag{6}$$

where $\alpha_d(t)$ is the virtual controller that needs to be devised in order to ascertain the vehicle's velocity necessary for maintaining the desired distance.

For speed control, the event triggering conditions for vehicle control are as follows:

$$\begin{aligned} u(t) &= \Upsilon(t_k), \forall t \in [t_k, t_{k+1}) \\ t_{k+1} &= \inf\{t > t_k \,||\beta(t)| \geq \mu|\Upsilon(t_k)| + \triangle\} \end{aligned} \tag{7}$$

where $\Upsilon(t_k)$ is the control signal transmitted to the actuator at discrete time points $t_k$, and $u(t)$ indicates the static input sustained by the actuator during the intervals between consecutive actuations. The positive constants $0 < \mu < 1$ and $\triangle$ function as coefficients. The expression $\beta(t) = \Upsilon(t) - u(t)$ captures the deviation between the real-time control input and the preceding control input. Furthermore, $\Upsilon(t)$ represents the control signal for each sampling period $h$.

Considering the above event triggering mechanism, when the preset threshold conditions (7) are met, the control signal of the actuator will be updated and the update time will be marked as $t_k(k \in z^+)$. During $t \in [t_k, t_{k+1}]$, the actuator maintains $\Upsilon(t_k)$. When (7) is violated again, the control signal of the actuator will be updated by $\Upsilon(t_{k+1})$, and actuator maintains $\Upsilon(t_k)$ until the next triggering moment arrives.

Based on the event triggering mechanism proposed above, the controller design process is given:

**Step 1:** Calculate the derivative of the spacing error $e_d(t)$ as $\dot{e}_d = v(t) - v^L(t)$. Select the Lyapunov function as:

$$V_d = \frac{1}{2}e_d^2 \tag{8}$$

Differentiating (8) and substituting (6) into it yields:

$$\begin{aligned} \dot{V}_d &= e_d\dot{e}_d = e_d\left(v(t) - \dot{p}^{\mathrm{L}}(t)\right) \\ &\leq e_d(v(t) - \alpha_d(t)) + e_d\alpha_d(t) - e_d\dot{p}^{\mathrm{L}}(t) \end{aligned} \tag{9}$$

where $\alpha_d$ is the virtual controller to be designed to obtain the vehicle speed required for distance control, specifically designed as:

$$\alpha_d(t) = -k_d e_d(t) + \dot{p}^{\mathrm{L}}(t) \tag{10}$$

Combing (10) and (9) yields:

$$\begin{aligned} \dot{V}_d &\leq e_d(v(t) - \alpha_d(t)) + e_d\left(-k_d e_d(t) + \dot{p}^{\mathrm{L}}(t)\right) - e_d\dot{p}^{\mathrm{L}}(t) \\ &\leq -k_d e_d^2(t) + e_d(v(t) - \alpha_d(t)) \end{aligned}$$

In order to avoid differentiation of the virtual controller $\alpha_d(t)$ during controller design, which can lead to complex interference terms, a nonlinear filter is designed. The specific form is:

$$\tau\dot{s} = -\mathrm{E} - \frac{\tau\hat{M}_d^2\mathrm{E}}{\sqrt{\hat{M}_d^2\mathrm{E}^2 + \sigma^2(t)}} - \tau e_d(t), \mathrm{E}(0) = \alpha_d(0) \tag{11}$$

where $\mathrm{E} = s - \alpha_d$ represents bounded boundary layer error; $\tau$ is the filtering time constant; $\hat{M}_d$ is an estimated value of $M_d$, while $M_d$ mainly represents bounded interference. Specific definitions will be provided in subsequent papers. $\sigma(t)$ is a positive function that satisfies $\lim_{t\to\infty}\int_0^t \sigma(s)\mathrm{ds} \leq \sigma_1 < +\infty$ with $|\dot{\sigma}| \leq \sigma_2 < +\infty$, where $\sigma(t)_1$ and $\sigma(t)_2$ are normal constants. The nonlinear filter designed in equation (11) compensates for the impact caused by boundary layer errors by introducing $-\frac{\tau\hat{M}_d^2\mathrm{E}}{\sqrt{\hat{M}_d^2\mathrm{E}^2+\sigma^2(t)}}$, thereby redefining the velocity error using the filtered signal

$$e_v(t) = v(t) - s(t) \tag{12}$$

*Remark 1.* The designed nonlinear filter (11) transforms the differential operation of the backstepping algorithm into simple algebraic operation, avoiding differentiation of the virtual controller (10).

**Step 2:** The strategy of a relative threshold, crafted through the fusion of an event-triggering mechanism and a controller, undergoes variations contingent upon the magnitude of the control signal.

From (7), during $[t_k, t_{k+1})$, it is clear that $|\beta(t)| \geq \mu|\Upsilon(t_k)| + \triangle$. Then, there are two situations:

- $\Upsilon(t_k) > 0$. In this situation, $\mu\Upsilon(t_k) - \leq \Upsilon(t) - \Upsilon(t_k) \leq -\mu\Upsilon(t_k) + \triangle$. It can be inferred that $\Upsilon(t) - \Upsilon(t_k) = \varsigma(\mu\Upsilon(t_k) + \triangle)$, where $-1 \leq \varsigma \leq 1$.
- $\Upsilon(t_k) < 0$. In this situation, $-\mu\Upsilon(t_k) - \leq \Upsilon(t) - \Upsilon(t_k) \leq -\mu\Upsilon(t_k) + \triangle$. It can be inferred that $\Upsilon(t) - \Upsilon(t_k) = \varsigma(\mu\Upsilon(t_k) - \triangle)$, where $-1 \leq \varsigma \leq 1$.

According to above two situations, we have $\Upsilon(t) - \Upsilon(t_k) = \varsigma_1\mu\Upsilon(t_k) + \varsigma_2\triangle$, where $\varsigma_1$ and $\varsigma_2$ satisfy $\varsigma_1 = \varsigma_2 = \varsigma$ when $\Upsilon(t) \geq 0$; $\varsigma_1 = \varsigma$ and $\varsigma_2 = -\varsigma$ when $\Upsilon(t) \leq 0$.

Define $\Upsilon(t) = (1 + \varsigma_1\mu)\Upsilon(t_k) + \varsigma_2$, the control input is:

$$u(t)=\Upsilon(t_k),\forall t\in[t_k,t_{k+1}) \tag{13}$$

Next, $u(t)$ is formulated as follows:

$$u(t)=\frac{\Upsilon(t)}{1+\varsigma_1\mu}-\frac{\varsigma_2\triangle}{1+\varsigma_1\mu} \tag{14}$$

Differentiating $e_v(t)$ yields:

$$\begin{aligned}\dot{e}_v(t)=&\frac{\Upsilon(t)}{1+\varsigma_1\mu}-\rho-W^{*\mathrm{T}}\Psi(\bar{x})-\varepsilon(\bar{x})+\frac{\mathrm{E}}{\tau}+\\&\frac{\hat{M}_d^2\mathrm{E}}{\sqrt{\hat{M}_d^2\mathrm{E}^2+\sigma^2(t)}}+e_d(t)\end{aligned} \tag{15}$$

where $\rho=-\frac{\varsigma_2\triangle}{1+\varsigma_1\mu}$, $\phi=\sup_{t\geq0}|\rho|$.

Define Lyapunov function:

$$V_v=V_d+\frac{1}{2}e_v^2+\frac{1}{2\zeta_1}\tilde{\bar{W}}^2+\frac{1}{2\zeta_2}\tilde{\bar{\varepsilon}}^2+\frac{1}{2\zeta_3}\tilde{\phi}^2 \tag{16}$$

where $\bar{W}=\|W\|$, $\tilde{\bar{W}}=\bar{W}-\hat{\bar{W}}$, $\tilde{\bar{\varepsilon}}=\bar{\varepsilon}-\hat{\bar{\varepsilon}}$, and $\tilde{\phi}=\phi-\hat{\phi}$.

By differentiating equation (16) and substituting equation (15) into it, it can be obtained that:

$$\begin{aligned}\dot{V}_v\leq&-k_de_d^2(t)+e_d(v(t)-\alpha_d(t))+e_v\frac{\Upsilon(t)}{1+\varsigma_1\mu}+e_v\frac{\mathrm{E}}{\tau}+\\&e_v\frac{\hat{M}_d^2\mathrm{E}}{\sqrt{\hat{M}_d^2\mathrm{E}^2+\sigma^2(t)}}+e_ve_d(t)+\\&e_v\tanh\left(\frac{e_v}{\varpi(t)}\right)\frac{1}{2\vartheta}\|\Psi(\bar{x})\|^2W+e_v\tanh\left(\frac{e_v}{\varpi(t)}\right)\vartheta+\\&\left(\frac{1}{2\vartheta}\|\Psi(\bar{x})\|^2W+\vartheta\right)\kappa\varpi(t)+e_v\tanh\left(\frac{e_v}{\varpi(t)}\right)\bar{\varepsilon}+\\&\bar{\varepsilon}\kappa\varpi(t)+e_v\tanh\left(\frac{e_v}{\varpi(t)}\right)\phi+\phi\kappa\varpi(t)-\frac{1}{\zeta_1}\tilde{\bar{W}}\dot{\hat{\bar{W}}}-\\&\frac{1}{\zeta_2}\tilde{\bar{\varepsilon}}\dot{\hat{\bar{\varepsilon}}}-\frac{1}{\zeta_3}\tilde{\phi}\dot{\hat{\phi}}\end{aligned} \tag{17}$$

The adaptive law for design parameters is:

$$\begin{aligned}\dot{\hat{\bar{W}}}&=\zeta_1e_v\tanh\left(\frac{e_v}{\varpi(t)}\right)\frac{1}{2\vartheta}\|\Psi(\bar{x})\|^2-\zeta_1\varpi(t)\hat{\bar{W}}\\\dot{\hat{\bar{\varepsilon}}}&=\zeta_2e_v\tanh\left(\frac{e_v}{\varpi(t)}\right)-\zeta_2\varpi(t)\hat{\bar{\varepsilon}}\\\dot{\hat{\phi}}&=\zeta_3e_v\tanh\left(\frac{e_v}{\varpi(t)}\right)-\zeta_3\varpi(t)\hat{\phi}\end{aligned} \tag{18}$$

Therefore, the final control algorithm is

$$\begin{aligned}u(t)&=\frac{\Upsilon(t)}{1+\varsigma_1\mu}-\frac{\varsigma_2\triangle}{1+\varsigma_1\mu}\\\Upsilon(t)&=(1+\varsigma_1\mu)\mathcal{U}\\\mathcal{U}&=-k_ve_v-\tanh\left(\frac{e_v}{\varpi(t)}\right)\frac{1}{2\vartheta}\|\Psi(\bar{x})\|^2\hat{\bar{W}}-\\&\quad\tanh\left(\frac{e_v}{\varpi(t)}\right)\vartheta-\tanh\left(\frac{e_v}{\varpi(t)}\right)\hat{\bar{\varepsilon}}-\tanh\left(\frac{e_v}{\varpi(t)}\right)\hat{\phi}\\&\quad-\frac{\hat{M}_d^2\mathrm{E}}{\sqrt{\hat{M}_d^2\mathrm{E}^2+\sigma^2(t)}}-2e_d-\frac{\mathrm{E}}{\tau}\end{aligned} \tag{19}$$

Substituting the controller and adaptive law designed by equations (18) and (19) into equation (17) yields:

$$\begin{aligned}\dot{V}_v\leq&-k_de_d^2(t)-k_ve_v^2(t)+\mathrm{E}e_d(t)+\tilde{\bar{W}}\varpi(t)\hat{\bar{W}}+\\&\tilde{\bar{\varepsilon}}\varpi(t)\hat{\bar{\varepsilon}}+\tilde{\phi}\varpi(t)\hat{\phi}+\\&\left(\frac{1}{2\vartheta}\|\Psi(\bar{x})\|^2W+\vartheta+\bar{\varepsilon}+\phi\right)\kappa\varpi(t)\end{aligned} \tag{20}$$

### *3.2 Stability Analysis*

*Theorem 1.* Considering the vehicle dynamics system described in (1), applying virtual controller designed in (10), nonlinear filter designed in (11), adaptive law designed in (18), and controller designed in (19) can ensure that:

1. The following vehicle can asymptotically track the leading vehicle and ensure stable operation at the expected safe distance, i.e $\lim_{t\to\infty}e_d=p(t)-p^{\mathrm{L}}(t)+d\to0$;

2. The following vehicle can quickly respond to changes in the leader vehicle, and the speed error between the two vehicles can converge to zero, that is $\lim_{t\to\infty}\dot{p}^{\mathrm{L}}(t)-v(t)\to0$;

3. The closed-loop system exhibits boundedness in all its states, specifically, encompassing the vehicle's velocity $v(t)$, the control input $u(t)$, the virtual controller $\alpha_d(t)$, and the nonlinear filter $s(t)$, all of which remain within finite limits.

Proof: Define Lyapunov function

$$V=V_v+\frac{1}{2}\mathrm{E}^2+\frac{1}{2\beta}\tilde{M}_d^2 \tag{21}$$

By differentiating equation (21), it can be obtained that

$$\dot{V}=\dot{V}_v+\mathrm{E}\dot{\mathrm{E}}+\frac{1}{\beta}\tilde{M}_d\dot{\hat{M}}_d \tag{22}$$

where $\dot{\mathrm{E}}=-\frac{\mathrm{E}}{\tau}-\frac{\hat{M}_d^2\mathrm{E}}{\sqrt{\hat{M}_d^2\mathrm{E}^2+\sigma^2(t)}}-e_d(t)-B\left(v(t),\dot{p}^L,\ddot{p}^L\right)$; $B\left(v(t),\dot{p}^L,\ddot{p}^L\right)$ is bounded; define $\left|B\left(v(t),\dot{p}^L,\ddot{p}^L\right)\right|\leq M_d$, where $\tilde{M}_d=M_d-\hat{M}_d$.

Furthermore, it can be inferred that

$$\begin{aligned}\dot{V}\leq&-k_de_d^2(t)-k_ve_v^2(t)+\tilde{\bar{W}}\varpi(t)\hat{\bar{W}}+\tilde{\bar{\varepsilon}}\varpi(t)\hat{\bar{\varepsilon}}+\tilde{\phi}\varpi(t)\hat{\phi}\\&+\left(\frac{1}{2\vartheta}\|\Psi(\bar{x})\|^2W+\vartheta+\bar{\varepsilon}+\phi\right)\kappa\varpi(t)\\&+\mathrm{E}\left\{-\frac{\mathrm{E}}{\tau}-\frac{\hat{M}_d^2\mathrm{E}}{\sqrt{\hat{M}_d^2\mathrm{E}^2+\sigma^2(t)}}-e_d(t)-M_d\right\}+\\&\mathrm{E}e_d(t)-\frac{1}{\beta}\tilde{M}_d\dot{\hat{M}}_d\end{aligned} \tag{23}$$

Using Young's inequality, it yields

$$\begin{aligned}\varpi(t)\tilde{\bar{W}}\hat{\bar{W}}=&\varpi(t)\tilde{\bar{W}}\left(-\tilde{\bar{W}}+\bar{W}\right)\\=&-\varpi(t)\tilde{\bar{W}}^2+\varpi(t)\tilde{\bar{W}}\bar{W}\leq\frac{1}{2}\varpi(t)\bar{W}^2\\\varpi(t)\tilde{\bar{\varepsilon}}\hat{\bar{\varepsilon}}\leq&\frac{1}{2}\varpi(t)\bar{\varepsilon}^2\\\varpi(t)\tilde{\phi}\hat{\phi}\leq&\frac{1}{2}\varpi(t)\phi^2\end{aligned} \tag{24}$$

Substituting equation (24) into equation (23) and considering $\|\Psi(\bar{x})\| \leq \sqrt{\lambda}, \lambda > 0$, we have

$$\dot{V} \leq -k_d e_d^2(t) - k_v e_v^2(t) + \left\{ \left( \frac{1}{2\vartheta}\lambda W + \vartheta + \bar{\varepsilon} + \phi \right) \kappa + \frac{1}{2}\bar{W}^2 + \frac{1}{2}\bar{\varepsilon}^2 + \frac{1}{2}\phi^2 \right\} \varpi(t) - \frac{\mathrm{E}^2}{\tau} - \frac{\hat{M}_d^2 \mathrm{E}^2}{\sqrt{\hat{M}_d^2 \mathrm{E}^2 + \sigma^2(t)}} + M_d |\mathrm{E}| - \frac{1}{\beta}\tilde{M}_d \dot{\hat{M}}_d \tag{25}$$

Drawing upon Lemma 2, we can derive

$$M_d |\mathrm{E}| \leq \frac{\hat{M}_d^2 \mathrm{E}^2}{\sqrt{\hat{M}_d^2 \mathrm{E}^2 + \sigma^2(t)}} + \sigma(t) + \tilde{M}_d |\mathrm{E}| \tag{26}$$

By incorporating equation (26) into equation (25), we can derive

$$\dot{V} \leq -k_d e_d^2(t) - k_v e_v^2(t) + \left\{ \left( \frac{1}{2\vartheta}\lambda W + \vartheta + \bar{\varepsilon} + \phi \right) \kappa + \frac{1}{2}\bar{W}^2 + \frac{1}{2}\bar{\varepsilon}^2 + \frac{1}{2}\phi^2 \right\} \varpi(t) - \frac{\mathrm{E}^2}{\tau} + \sigma(t) - \frac{1}{\beta}\tilde{M}_d \left( \dot{\hat{M}}_d - \beta |\mathrm{E}| \right) \tag{27}$$

Design the adaptive law $\dot{\hat{M}}_d = \beta |\mathrm{E}|$, and define

$$\theta = \left( \frac{1}{2\vartheta}\lambda W + \vartheta + \bar{\varepsilon} + \phi \right) \kappa + \frac{1}{2}\bar{W}^2 + \frac{1}{2}\bar{\varepsilon}^2 + \frac{1}{2}\phi^2 \tag{28}$$

Therefore, we have

$$\dot{V} \leq -k_d e_d^2(t) - k_v e_v^2(t) + \theta\varpi(t) - \frac{\mathrm{E}^2}{\tau} + \sigma(t) \tag{29}$$

Integrating equation (29) on $[0, t]$ can obtain

$$V(t) \leq V(0) + \theta \int_o^t \varpi(\mathrm{w})\,\mathrm{dw} + \int_0^t \sigma(\mathrm{w})\,\mathrm{dw} - \int_0^t \left\{ k_d e_d^2(\mathrm{w}) + k_v e_v^2(\mathrm{w}) + \frac{\mathrm{E}^2(\mathrm{w})}{\tau} \right\} \mathrm{dw} \leq V(0) + \theta\varpi_1 + \sigma_1 \tag{30}$$

When (30) is satisfied, it represents $e_d, e_v, \mathrm{E}, \hat{\bar{W}}, \hat{\bar{\varepsilon}}, \hat{M}_d$ are bounded. Furthermore, it can be seen that $s, \alpha_d, u, v(t)$ are also bounded. In addition, from (30), we can derive

$$\int_0^t k_d e_d^2(\mathrm{w})\,\mathrm{dw} \leq V(0) + \theta\varpi_1 + \sigma_1$$
$$\int_0^t k_v e_v^2(\mathrm{w})\,\mathrm{dw} \leq V(0) + \theta\varpi_1 + \sigma_1$$
$$\int_0^t \frac{\mathrm{E}^2(\mathrm{w})}{\tau}\mathrm{dw} \leq V(0) + \theta\varpi_1 + \sigma_1 \tag{31}$$

In this case, using the Barbarat Lemma, it can be seen that $\lim_{t\to\infty} e_d \to 0$, $\lim_{t\to\infty} e_v \to 0$ and $\lim_{t\to\infty} \mathrm{E} \to 0$. As a result, the following vehicle is capable of adhering to the speed of the leading vehicle while sustaining the desired distance between them, ensuring safe operation. Importantly, the designed nonlinear filter suppresses the filtering error caused by traditional linear filters and improves control accuracy. The proof is end.

*Theorem 2.* The existence time $t^* > 0$ makes the $t_{k+1} - t_k \geq t^*, \forall k \in z^+$ exist, and the Zeno phenomenon can be avoided.

Proof: By definition $\beta(t) = \Upsilon(t) - \Upsilon(t_k), \forall t \in [t_k, t_{k+1})$, there exists

$$\frac{d}{dt}|\beta(t)| = \frac{d}{dt}(\beta(t) * \beta(t))^{1/2} = \mathrm{sign}(\beta(t))\,\dot{\beta}(t) \leq \left|\dot{\Upsilon}(t)\right| \tag{32}$$

Hence, all signals within the closed-loop system remain confined within finite bounds and $\beta(t_k) = 0$, $\lim_{t\to t_{k+1}} \beta(t_k) = \Delta v(t)$ is differentiable, so there must be a normal number $Y > 0$ that satisfies $\left|\dot{\Upsilon}(t)\right| \leq Y$. To ensure that the minimum boundary $t^*$ of the execution time interval must meet $t^* \geq \frac{\Delta}{Y} > 0$, therefore the Zeno phenomenon is ruled out.

## 4. SIMULATIONS

To verify the effectiveness of designed event-triggered ACC on vehicles under uncertain nonlinear driving resistance, this section assumes that the driving resistance of the vehicle is time-varying, mainly manifested in the vehicle running on different slopes (before 100s, the road slope angle is 2°, after 100s, the road slope angle becomes 3°). $C_D$ and $C_R$ are assumed as time-varying values.

Set the operating speed of the leader vehicle to the Economic Commission for Europe (ECE) test speed curve (Liu et al., 2023). The vehicle initial states are: $p(0) = 0m$, $v(0) = 0m/s$, $p^L(0) = 10m$.

Table 1. Parameters of vehicle

| Parameters | Value | Parameters | Value |
|---|---|---|---|
| $m$/kg | $1250 + 250\sin(t)$ | $\rho/\left(\mathrm{N}\cdot\mathrm{s}^2\cdot\mathrm{m}^{-4}\right)$ | 1.2258 |
| $C_D$ | $0.35 + 0.05\sin(t)$ | $g/\left(\mathrm{m/s}^2\right)$ | 9.8 |
| $C_R$ | $0.018 + 0.002\sin(t)$ | $A/\mathrm{m}^2$ | 2.2 |

The designed ACC parameters based on neural network approximation are selected as follows: $k_d = 20$, $\tau = 0.01$, $\zeta_1 = 20$, $\zeta_2 = 2$, $\zeta_3 = 20$, $k_v = 20$, $\varpi(t) = 0.01e^{-0.001t}$, $\vartheta = 1$, $\beta = 0.5$, $\mu_l = [-1, -0.5, 0, 0.5, 1]$, $\chi_l = [0.5, 0.5, 0.5, 0.5, 0.5]$, $\varsigma_1 = 0.25$, $\mu = 0.01$, $\triangle = 0.05$. The execution interval is set to 0.001s and 0.01s respectively.

Figure 3 presents the simulation results of the proposed algorithm with 0.001s sampling time interval. Figure 3 (a) demonstrates high control accuracy, with a distance error below 0.03 m. Figure 3 (b) shows that the follower vehicle accurately tracks the leader's speed across acceleration, deceleration, and cruising phases. The control input profile in Figure 3 remains stable. The event-triggering mechanism in Figure 3 (d) significantly reduces actuator updates. With only 19,757 triggers (a reduction of 170,243 from 190,000), it achieves an 89.6% saving, enhancing efficiency.

Figure 4 presents the simulation results of the proposed algorithm with with a sampling interval of 0.01 seconds. Figure 4 (a) shows that the distance error of the vehicles does not exceed 0.3m. Figure 4 (b) shows that the follower vehicle accurately tracks the leader's speed. Figures 4 (c) illustrates the control input profiles of the vehicle. Figure 4 (d) shows the event triggering interval. The actuator triggered 1533 times, saving 91.93%.

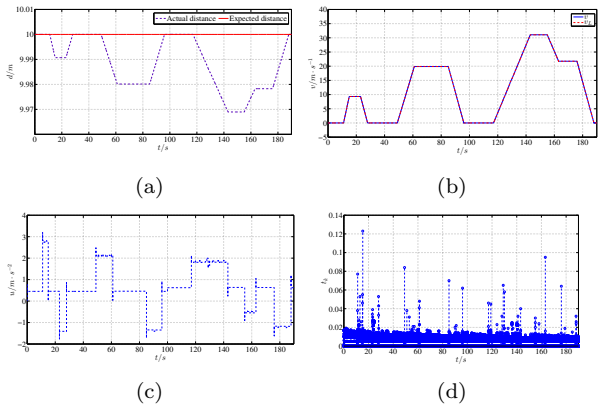



Fig. 3. Simulation results of designed algorithm with 0.001s sampling time interval: (**a**) Distance. (**b**) Speed. (**c**) Control input. (**d**) Event triggering interval.

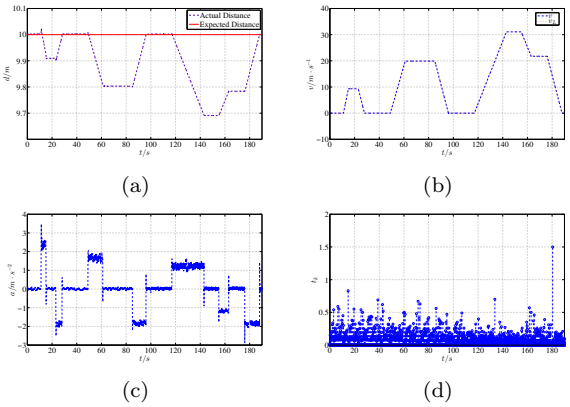



Fig. 4. Simulation results of designed algorithm with 0.01s sampling time interval: (**a**) Distance. (**b**) Speed. (**c**) Control input. (**d**) Event triggering interval.

## 5. CONCLUSIONS

This paper designs an event triggered ACC algorithm. The designed algorithm does not require an accurate vehicle model, and utilizes the vehicle's state information to learn the uncertain driving resistance online. Only one adaptive learning of network weights is required. In addition, by introducing event triggered control technology, the designed algorithm can significantly reduce the execution frequency of the actuator, and the stability of the system is analyzed through Lyapunov stability theorem. Through comparative simulation verification, it can be concluded that the control accuracy of the designed algorithm is related to the sampling frequency, and can be balanced between control accuracy and computational efficiency.

## REFERENCES


Derbel, O., Peter, T., Zebiri, H., Mourllion, B., and Basset, M. (2013). Modified intelligent driver model for driver safety and traffic stability improvement. *IFAC Proceedings Volumes*, 46(21), 744–749.

Ganji, B., Kouzani, A.Z., Khoo, S.Y., and Shams-Zahraei, M. (2014). Adaptive cruise control of a hev using sliding mode control. *Expert systems with applications*, 41(2), 607–615.

Izci, D., Ekinci, S., Kayri, M., and Eker, E. (2022). A novel improved arithmetic optimization algorithm for optimal design of pid controlled and bode's ideal transfer function based automobile cruise control system. *Evolving Systems*, 13(3), 453–468.

Ju, P. and Song, J. (2023). An improved advanced driver-assistance system: model-free prescribed performance adaptive cruise control. *Applied Sciences*, 13(20), 11499.

Lin, Y., McPhee, J., and Azad, N.L. (2020). Comparison of deep reinforcement learning and model predictive control for adaptive cruise control. *IEEE Transactions on Intelligent Vehicles*, 6(2), 221–231.

Liu, X., Yan, M., Yang, P., and Song, J. (2023). Observer-based actuator fault detection and robust tolerant control for vehicle platoons. *International Journal of Control, Automation and Systems*, 21(4), 1175–1186.

Marzbanrad, J. and Karimian, N. (2011). Space control law design in adaptive cruise control vehicles using model predictive control. *Proceedings of the Institution of Mechanical Engineers Part D Journal of Automobile Engineering*, 225(7), 870–884.

Milanés, V., Villagrá, J., Godoy, J., and González, C. (2011). Comparing fuzzy and intelligent pi controllers in stop-and-go manoeuvres. *IEEE Transactions on Control Systems Technology*, 20(3), 770–778.

Park, C. and Lee, H. (2017). A study of adaptive cruise control system to improve fuel efficiency. *International Journal of Environmental Pollution and Remediation*, 5, 1–15.

Sawant, J., Chaskar, U., and Ginoya, D. (2020). Robust control of cooperative adaptive cruise control in the absence of information about preceding vehicle acceleration. *IEEE Transactions on Intelligent Transportation Systems*, 22(9), 5589–5598.

Song, J., Yan, M., Ju, Y., and Yang, P. (2019). Nonlinear gain feedback adaptive dsc for a class of uncertain nonlinear systems with asymptotic output tracking. *Nonlinear Dynamics*, 98(3), 2195–2210.

Xu, Y., Zhou, Q., Li, T., and Liang, H. (2019). Event-triggered neural control for non-strict-feedback systems with actuator failures. *IET Control Theory & Applications*, 13(2), 171–182.

Yang, P., Chen, X., Zhao, X., and Yan, M. (2022). Fixed time event-triggered tracking control for interconnected nonlinear uncertain systems: An observer-based approach. *International Journal of Control, Automation and Systems*, 20(8), 2641–2654.

Yu, L. and Wang, R. (2022). Researches on adaptive cruise control system: A state of the art review. *Proceedings of the Institution of Mechanical Engineers, Part D: Journal of Automobile Engineering*, 236(2-3), 211–240.

Zhang, J. and Ioannou, P.A. (2006). Longitudinal control of heavy trucks in mixed traffic: Environmental and fuel economy considerations. *IEEE Transactions on Intelligent Transportation Systems*, 7(1), 92–104.

Zhang, Y. and Song, J. (2023). Model-free robust back-stepping adaptive cruise control. *International Journal of Aerospace Engineering*, 2023.

Zhu, X., Yan, M., Panpan, Y., and Yongtao, L. (2024). Computation of the exact time delay margin for vehicle platoon under generic communication topologies. *Journal of Traffic and Transportation Engineering (English Edition)*, 11(4).